TRAJECTORIES: ISOBARIC, ISENTROPIC AND ACTUAL

Edwin F. Danielsen

University of Washington

(Original manuscript received 12 August 1960; revised manuscript received 10 February 1961)

ABSTRACT

Vertical and horizontal deviations between an air trajectory and isobaric and isentropic trajectories are presented in a convenient form for order-of-magnitude comparisons and interpretation. Also, an objective method for computing isentropic trajectories is developed which is based on the total-energy equation.

1. Introduction

As meteorology proceeds from pressure prediction to weather prediction, more attention will, by necessity, be directed to integrated three-dimensional motions of the air. These motions, or trajectories, can be computed from the conventional pressure analyses, but vertical motions add complexities and uncertainties not only in the vertical component of the trajectories but in the horizontal components as well. Isentropic analyses offer an alternative procedure for trajectory computations. By directly incorporating the vertical motions and velocity shears, they eliminate the major sources of error of the isobaric method, but another source of error is introduced because it is necessary to evaluate the diabatic temperature change. This is difficult to evaluate, but usually the order of magnitude of the change can be determined.

Since the need is to determine the three-dimensional trajectories of the air, it is advantageous to express the vector errors between an air trajectory and isobaric and isentropic trajectories as a function of vertical velocities and diabatic rates to enable order-of-magnitude comparisons. In order that these errors may be isolated from computational errors, it is helpful to postulate an isentropic balloon, an analogue of the existing isobaric balloon. The trajectories of the two balloons will then represent accurately computed isobaric and isentropic trajectories.

2. Method

If an isobaric balloon and an isentropic one are released from the same point, they will in general trace out different trajectories from the air initially adjacent to them, thereby generating three different position vectors. The difference vector between either balloon's position vector and the air's position vector can then be expressed in the following form,

$$\mathbf{r}'_{p,\theta} = \int\int\left[(W - W_{p,\theta})\frac{\partial V}{\partial z} + \left(r'\frac{\partial}{\partial r} + z'\frac{\partial}{\partial z} + \cdots\left(\frac{dV}{dt}\right)\right)\right](dt)^2 \quad (1)$$

$$z'_{p,\theta} = \int\left[(W - W_{p\,\theta}) + \left(r'\frac{\partial}{\partial r} + z'\frac{\partial}{\partial z} + \cdots\right)\right]dt, \quad (2)$$

where $\mathbf{r}'$ is the horizontal component of the difference vector and z' is the vertical component. With the subscript p, it points from the isobaric balloon to the air parcel, with θ from the isentropic balloon to the air parcel. r' is the magnitude of $\mathbf{r}'$, V and W are the horizontal and vertical velocity of the air, and W_p and W_θ are the vertical velocities of the respective balloons. In (1) and (2), the horizontal acceleration, vertical wind shear and vertical velocity of the air at the position of the air parcel have been replaced by their Taylor expansions about the position of the balloon. Higher-order terms in the expansion are denoted by the dots. All terms in (1) and (2) are therefore evaluated at the position of the balloon, so it is possible to draw some rather definite conclusions about the three types of trajectories from the magnitudes of the terms and their correlations.

If the actual trajectory is compared to the isobaric, it is evident that both horizontal and vertical deviations between the trajectories are initiated by a vertical velocity relative to the pressure surface. Whenever $W - W_p$ is non-zero, z_p' will become non-zero upon further integration. Then, if $\mathbf{r}_p'$ is to remain zero (the air and balloon remain in vertical alignment), it is necessary that $\partial V/\partial z$ and $(\partial/\partial z)(dV/dt)$ are both zero, which is equivalent to a requirement of barotropy.

This condition is generally incompatible with the former condition that $W - W_p \neq 0$. Synoptic experience, dish-pan experiments and theoretical models indicate that large-scale vertical motions correlate positively with temperature advection. A positive correlation would be expected during amplification of a baroclinic disturbance and during steady-state conditions to offset the frictional dissipation of kinetic energy. Stated another way, a positive correlation implies that the local temperature change is less than the advective change. This has been frequently observed in the troposphere and lower stratosphere.

If vertical motion correlates with temperature advection, it is definite that r_p' will become non-zero. If the correlation is positive, it can be deduced with confidence that r_p' will develop a component to the right of the isobaric balloon's velocity when the air is descending or ascending. This follows because with advection the velocity shear has a component orthogonal to the velocity. With cold advection the component is directed to the left, but the negative vertical velocity directs the product to the right. The product remains the same with warm advection because both terms reverse sign. The direction of the product will be denoted by the unit vector $\boldsymbol{n}$.

As the deviations r_p' and z_p' increase, all three terms in (1) and (2) may contribute to their rate of change. It can be shown, although the argument is a bit lengthy and will therefore only be outlined, that all three terms frequently act in the same sense because of the correlation of geostrophic departures, vertical motion and velocity shears in a baroclinic fluid. The argument depends on the following set of probable conditions associated with regions of vertical motion.

1. Synoptic studies indicate that curvature accelerations usually exceed speed accelerations.

1a. Largest horizontal derivative of accelerations is then normal to the wind and directed along $\boldsymbol{n}$.

2. Pressure systems tilt with height with cyclonic accelerations located above anticyclonic ones, and vice versa.

2a. The product of vertical deviations and largest component of vertical derivative of acceleration is then also along $\boldsymbol{n}$.

3. A large component of velocity advection into pressure surfaces is also along $\boldsymbol{n}$.

Under these conditions, the rate of change of the deviations is proportional to the deviations and the actual air trajectory rapidly diverges from the constant pressure trajectory. Such a rapid growth would require retaining higher-order terms in the Taylor expansion or constructing the air's trajectory from segments of isobaric trajectories on several pressure surfaces.

To compare the magnitudes of r_p', z_p' with r_θ' and z_θ', it is convenient to convert the vertical velocities relative to the isentropic surface to diabatic rates. The dominant terms in (1) and (2) become

$$W - W_\theta = \frac{\partial z}{\partial \theta}\frac{d\theta}{dt} \qquad (W - W_\theta)\frac{\partial V}{\partial z} = \frac{\partial V}{\partial \theta}\frac{d\theta}{dt}$$

which can be readily compared to

$$W - W_p \qquad (W - W_p)\frac{\partial V}{\partial z}.$$

In regions of active development, values of ± 5 cm sec^{-1} or 4 km per 24 hr have been observed for $W - W_p$. If the vertical motion relative to the isentropic surface was the same magnitude and the stability ranged from 1 to 10 deg per 1000 ft, a $d\theta/dt = \pm 14$ to 140 deg per 24 hr would be required. This is one to two orders of magnitude greater than the diabatic rates calculated and observed for the free atmosphere in the absence of phase changes. If the above-mentioned vertical motion is combined with a shear of 10 m sec^{-1} km^{-1} which acts over a twelve-hour period, the magnitude of r_p' would be 930 km or approximately 8.5 deg of lat. For the same shear, a diabatic rate of 1 deg K per 12 hr would generate an r_θ' of 65 km or approximately 0.6 deg of lat corresponding to the aforementioned lower stability and 0.06 deg of lat with the larger stability. Under these conditions, the isentropic balloon stays close enough to the air parcel to neglect the higher-order terms in the Taylor expansion. As the stability approaches zero, z_θ' and r_θ' approach infinity, but this has physical significance because vertical mixing will then destroy the identity of the air parcel.

3. Examples

Three examples illustrating differences between isobaric and isentropic trajectories are presented in figs. 1 to 6. Both horizontal and vertical differences are incorporated in fig. 1. In the remaining examples, they are presented separately as projections on maps and pseudo-adiabatic diagrams. The isobaric trajectories are constructed from the observed winds. The distance traveled is equal to the product of a twelve-hour interval and the linear mean of the initial and final wind speeds. In these examples, no cross-contour flow is evident along the path of the isobaric trajectory, so the displacements are made parallel to the contours. If the wind and consequently the velocity of the isobaric balloon are actually at an angle to the contours, these trajectories will differ slightly from the trajectory of the isobaric balloon. An angle less than five degrees can hardly be detected. By using five degrees as a probable value and a mean speed of 30 m per sec, the difference after twelve hours would

be one degree of latitude. All the isentropic trajectories are constructed by using the method developed in the next section which incorporates the speed accelerations of the air.

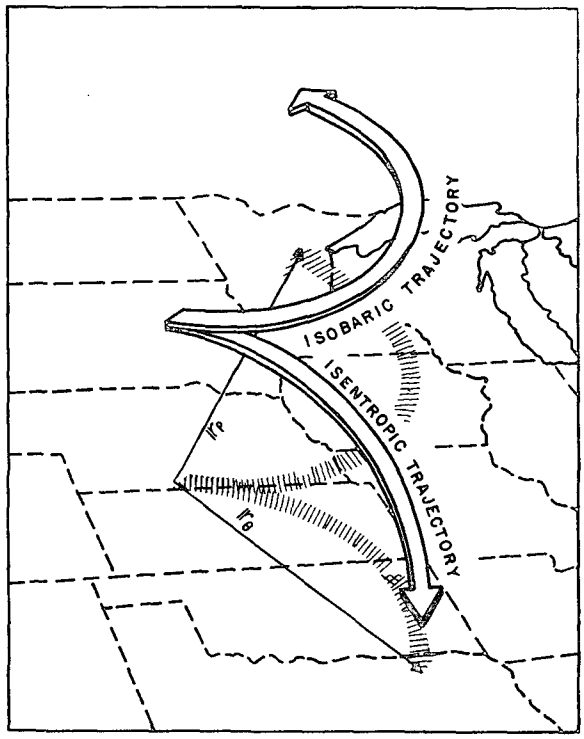

FIG. 1. A comparison of twelve-hour isobaric and isentropic trajectories originating at 700 mb at 0300 GCT 28 March 1956. Terminal pressure of the 290K isentropic trajectory is 880 mb. Horizontal deviation is 1300 ± 200 km.

All trajectories are of the subsidence type to eliminate large diabatic effects of phase changes. Horizontal and vertical differences are large; therefore, it might be tempting to dismiss them as unrealistic. To counter this temptation, supporting evidence is offered by including portions of the sounding from the nearest radiosone, calculations of initial and final potential vorticities, and comparisons of initial and final moisture contents. If diabatic rates are small, the conservation of potential vorticity and mixing ratio are necessary conditions, although not sufficient conditions that the trajectories are reliable. The potential vorticity is the product of the stability, $\partial\theta/\partial p$, and the vertical component of vorticity, $\eta_\theta = \zeta_\theta + f$, where the relative vorticity, ζ_θ, is determined from the horizontal winds on the isentropic surface and f is the vertical component of the earth's vorticity.

In fig. 1, of example one, a twelve-hour 290K isentropic trajectory starting at 700 mb and terminating at 880 mb is drawn in perspective to emphasize how drastically it departs from a 700-mb trajectory starting at the same point. The curvatures are of the opposite sign, horizontal separation (1,300 ± 200 km) exceeds the distance traveled, and vertical velocity averages 7 cm sec^{-1} for the first six hours and 4.3 cm sec^{-1} for twelve hours. The isentropic trajectory is the second half of a previously reported 24-hr trajectory [see Danielsen (1959) for the complete trajectory and 290K isentropic charts] which originates at 535 mb over Great Falls, Montana at 1500 GCT 27 March 1956. Note similarity of this trajectory to the 290K trajectories constructed by Palmen and Neuton (1951) fig. 8. 290K is the potential temperature at the base of a thin layer slightly more stable than its adjacent layers. The water vapor is close to saturation with respect to ice. Conditions in this layer at Great Falls are presented at the top of fig. 2.

As the air moves southeastward, it increases in speed and descends to the 700-mb level over south-central Nebraska. This is the origin of the trajectories in fig. 1. At this time, 0300 GCT 28 March, the closest radiosonde observation was made at North Platte. It contains a stable layer very similar to the one observed twelve hours earlier at Great Falls, but the potential temperature at its base is one degree higher. After assuming this represents the same layer its stability was combined with the vorticity on the 290K surface to determine the calculations associated with North Platte in fig. 2. A comparison of Great Falls and North Platte data indicate the stability, vorticity and potential vorticity are all approximately conserved during the motion.

By way of contrast as the air descends, decelerates and curves anticyclonically from southern Nebraska to northeastern Texas, the vorticity decreases by a factor of three. Radiosonde data from Forth Worth at 1500 GCT 28 March indicate the stability has increased by a factor of three, so the potential vorticity is once again approximately conserved. This suggests that the trajectory is reliable, and additional support is given by the unusual moisture distribution at Fort Worth. At 290K, in the thin stable layer, the air is too dry to obtain a relative-humidity measurement from the radiosonde equipment. The limiting value at this temperature is 13 per cent. If the mixing ratios at Great Falls and North Platte are conserved during descent, the relative humidities are well below this limiting value as illustrated by the dashed lines at the left of fig. 2. If, as the evidence suggests, the dry air in the stable layer at 880 mb over northeastern Texas was at 535 mb over Montana 24 hr earlier, then a diabatic cooling of 1K per 24 hr is indicated. An error in the trajectory due to diabatic changes is consequently negligible.

The second example, figs. 3 and 4, is less dramatic than the first, although the average vertical motion, 7.4 cm sec^{-1} per 12 hr, is larger. The isentropic trajectory is at 30C or 30K. It starts at 436 mb over Omaha, Nebraska at 0000 GCT 2 January 1958 and

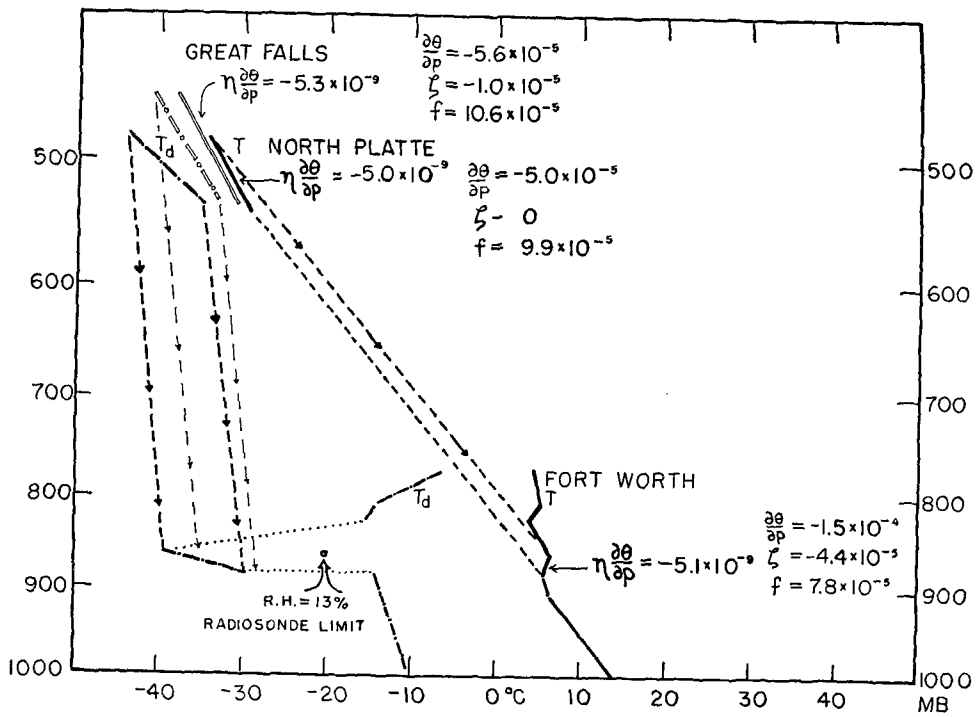

FIG. 2. Segments of soundings from Great Falls, Montana at 1500 GCT 27 March 1956, from North Platte, Nebraska at 0300 GCT 28 March 1956 and from Forth Worth, Texas at 1500 GCT 28 March 1956. All values of stability, vorticity and potential vorticity are expressed in cgs units.

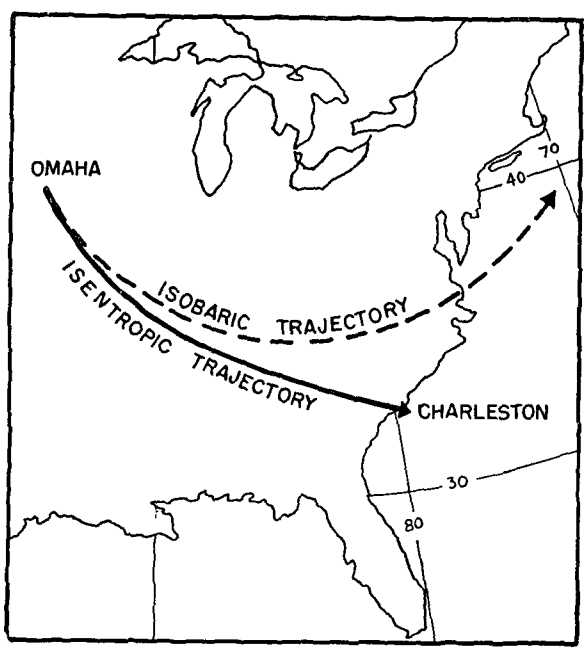

FIG. 3. A comparison of twelve-hour isobaric and isentropic trajectories originating at 435 mb at 0000 GCT 2 January 1958. Terminal pressure of 303K isentropic trajectory is 666 mb. Horizontal deviation is 1100 ± 200 km. Average vertical velocity is -7.4 cm sec^{-1}.

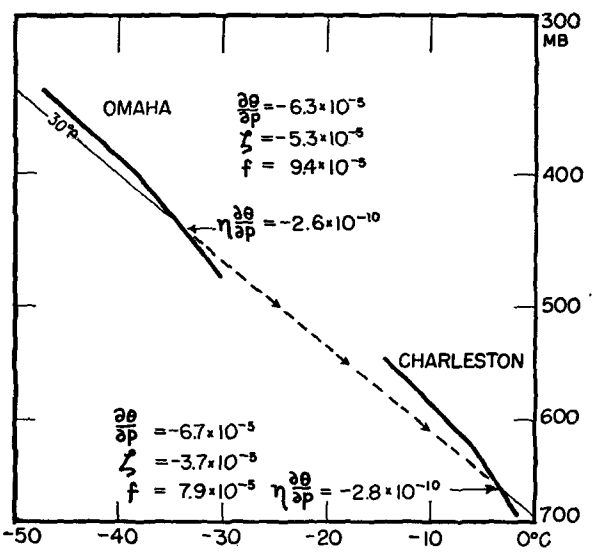

FIG. 4. Segments of soundings from Omaha, Nebraska at 0000 GCT 2 January 1958 and from Charleston, South Carolina at 1200 GCT 2 January 1958. All values of stability, vorticity and potential vorticity are expressed in cgs units.

descends to 665 mb over Charleston, South Carolina in twelve hours. The isobaric trajectory was constructed from the 400-mb data. Curvatures of both trajectories are positive, but that of the isentropic trajectory is approaching zero at Charleston. The horizontal deviation at the end of the period is approximately 1100 km. The stability, vorticity and potential vorticity are all approximately conserved. The relative humidity at both Omaha and Charleston was too low to be measured.

In the third example, a stratospheric trajectory starting in Northwestern Montana at 1500 27 March 1956 is illustrated in figs. 5 and 6. The isentropic trajectory which was computed backward in time from Denver, Colorado at 0000 GCT 28 March 1956 is at 320K. The isobaric is at 250 mb. Along the isentropic trajectory from Montana to Denver, a speed increase from 25 to 35 m sec^{-1} and a cross stream function flow is calculated by using the method in the next section (see accelerated trajectory in fig. 5) Because no cross-contour flow is incorporated in the isobaric trajectory, these trajectories may underestimate r_p'. If the air at the successive positions of the isobaric balloon is accelerating in speed as is the air on the isentropic surface, then the deviation would be larger, approximately the r_p' between the isentropic trajectory parallel to ψ (see fig. 5) and the isobaric trajectory.

As found by referring back to (1), the uncertainty in this example is in the spatial derivatives of the acceleration of the air. Since the air does not pass the trough during the twelve hours, it is probable that, on the average, speed acceleration occurs and r_p' lies between the two values indicated above. On the other hand, the isobaric trajectories of the two earlier examples originate west of the trough and terminate east of the trough. It is probable that speed deceleration occurs on their respective pressure surfaces west of the trough and that speed acceleration occurs east of the trough so that the average speed accelerations along the isobaric trajectories would be small and the r_p''s are representative. It should be noted that this uncertainty could be eliminated if the isobaric trajectories could be constructed from stream-line analyses on the pressure surfaces, but, except for regions of large divergence and convergence, the streamlines are usually as uncertain as are the contours.

In the case of example three, potential vorticities are not computed because of the large uncertainty in the initial vorticity. As can be seen in fig. 6, the stability is approximately conserved between Spokane, Washington and Denver, Colorado. It is concluded, after having analyzed the vertical cross sections, that the stability at Spokane at 1500 GCT 27 March 1956 is representative of the stability at the beginning of the trajectory.

The sounding from Great Falls, Montana at 1500 GCT 27 March 1956 is included in fig. 6 because it is very close to the origin of the 300K trajectory that terminated at Denver. This is an excellent example of the complex non-linear variations of temperature that are produced by different advections of pre-existing stabilities.

4. Method of constructing trajectories

Tracing the trajectory of the air is equivalent to tracing the three-dimensional motion of an infinitesimal open system which has no net mass flux across

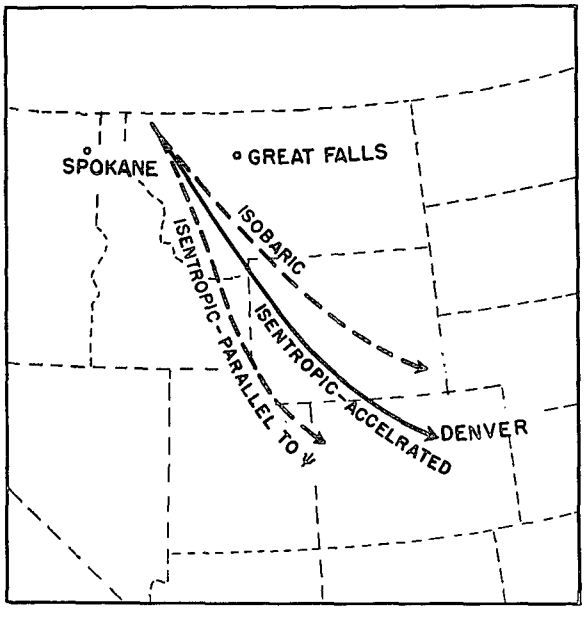

FIG. 5. A comparison of twelve-hour trajectories originating at 250 mb at 1500 GCT 27 March 1956. Terminal pressure of 320K isentropic trajectory is 293 mb.

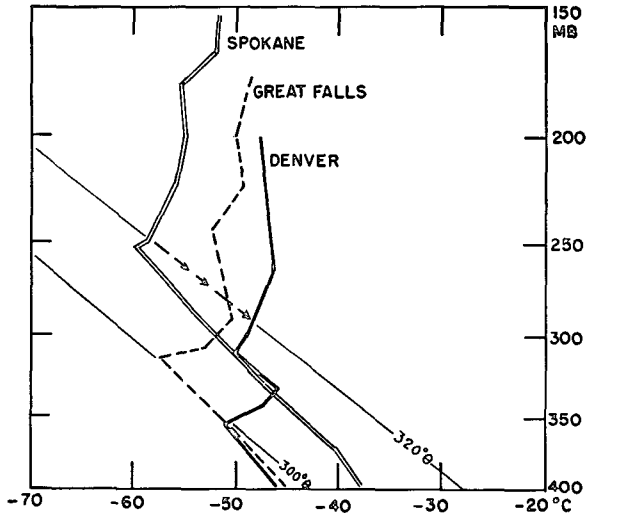

FIG. 6. Soundings from Spokane, Washington and Great Falls, Montana at 1500 GCT 27 March 1956 and from Denver, Colorado at 0300 GCT 28 March 1956.

its boundaries. Addition of the thermodynamic and mechanical energy equations as shown by Brunt (1941) yields the appropriate energy equation for this system. One form for this equation is

$$\frac{dq}{dt} + \alpha \frac{\partial p}{\partial t} = \frac{d}{dt}\left[c_p T + gZ + \frac{V^2}{2}\right] \tag{3}$$

where q is the heat transfered per unit mass, c_p is the specific heat at constant p, g is the acceleration of gravity, and α, T, Z, V are the specific volume, temperature, height and speed of the system.

Eq. (3) can be expressed in terms of the isentropic stream function, which is defined by

$$\psi \equiv c_p T + gZ. \tag{4}$$

It can be shown that the second term transforms to

$$\alpha \frac{\partial p}{\partial t} = \frac{\partial \psi}{\partial t_\theta} - \left[\alpha \frac{\partial p}{\partial z} + g\right] \frac{\partial z}{\partial t_\theta}. \tag{5}$$

Under the hydrostatic approximation, the bracketed term vanishes. Substituting (4) and (5) into (3) yields

$$\frac{dq}{dt} + \frac{\partial \psi}{\partial t_\theta} = \frac{d\psi}{dt} + \frac{d}{dt}\left(\frac{V^2}{2}\right), \tag{6}$$

but it must be recognized that under the hydrostatic approximation the kinetic energy of the vertical motion must be neglected.

If all the total derivatives are expanded with θ as an explicit variable, (6) becomes

$$c_p \frac{T}{\theta}\frac{d\theta}{dt} + \frac{\partial \psi}{\partial t_\theta} = \frac{d\psi}{dt_\theta} + \frac{\partial \psi}{\partial \theta}\frac{d\theta}{dt} + \frac{d}{dt}\left(\frac{V^2}{2}\right) + \frac{\partial}{\partial \theta}\left(\frac{V^2}{2}\right)\frac{d\theta}{dt}. \tag{7}$$

Two of the diabatic terms cancel identically because under the hydrostatic assumption $\partial\psi/\partial\theta = c_p(T/\theta)$. If the remaining terms are integrated, the result is

$$\int \frac{\partial \psi}{\partial t_\theta} dt = (\psi_2 - \psi_1)_\theta + \left(\frac{V_2^2 - V_1^2}{2}\right)_\theta + \overline{\frac{\partial}{\partial \theta}\left(\frac{V^2}{2}\right)}(\theta_2 - \theta_1) \tag{8}$$

where subscript 1 indicates the initial values and 2 indicates the final values. The first term represents that portion of the change in enthalpy and potential energy of the system that is not converted into kinetic energy. The third and fourth terms express the total change in the kinetic energy of the horizontal wind. This equation is in a convenient form for direct application to the construction of trajectories on isentropic charts. The second and third terms are only functions of the initial and final data which is a distinct advantage because of the twelve-hour interval between data. The first term must be approximated. The best method of approximation is to first obtain the local change in ψ over the entire field by graphical subtraction of two successive ψ analyses and then sum the local change along the proposed trajectory. An alternative method is to replace the first term by

$$\int \frac{\partial \psi}{\partial t_\theta} dt \simeq \frac{\Delta\psi_1 + \Delta\psi_2 + 2\Delta\psi_M}{4} \tag{9}$$

where Δ denotes the twelve-hour difference at a fixed point and M denotes the position of the system at the midtime. The fourth term cannot be measured directly, but it is sometimes possible to correct for the diabatic change by a method of successive approximations.

As a first approximation, this term is neglected. If the trajectory indicates a sufficient decrease in pressure to condense out m grams of water vapor, the second approximation can include the increase of θ due to the release of latent heat. A new trajectory will be obtained which will in turn indicate a different m. The process is then repeated until a limiting value is reached.

In constructing the trajectory, it is advantageous to start at a data point; then ψ and V are known. The objective then is to determine a final point such that the following approximate equations are satisfied; *i.e.*,

$$\psi_2 - \psi_1 + \frac{V_2^2}{2} - \frac{V_1^2}{2} \simeq \frac{\Delta\psi_2 + \Delta\psi_1 + 2\Delta\psi_M}{4} \tag{10}$$

$$D \simeq \frac{V_2 + V_1}{2}\Delta t \tag{11}$$

where D is the distance traveled by the system in the time Δt and it is understood that all values are at constant θ.

It may happen that more than one point satisfies these equations. It is characteristic of the anticyclonic side of the jet that points on a line segment will all satisfy them. This follows because the gradient of ψ and V are negatively correlated. Any point on the line is then equally probable. Presumably, this indeterminency could be eliminated by using the gradient-wind equation which is independent of the energy equation. It should apply at all points along the trajectory and could be specifically applied to the end point. However, the gradient of ψ must be evaluated, and it appears doubtful that it can be determined with sufficient accuracy to remove the indeterminency.

As an aid in the computations, it is advantageous to construct a graph of the change in kinetic energy per unit mass with V_1 and V_2 as the coordinates and draw isopleths on the graph for the same interval used in analyzing ψ on the isentropic chart.

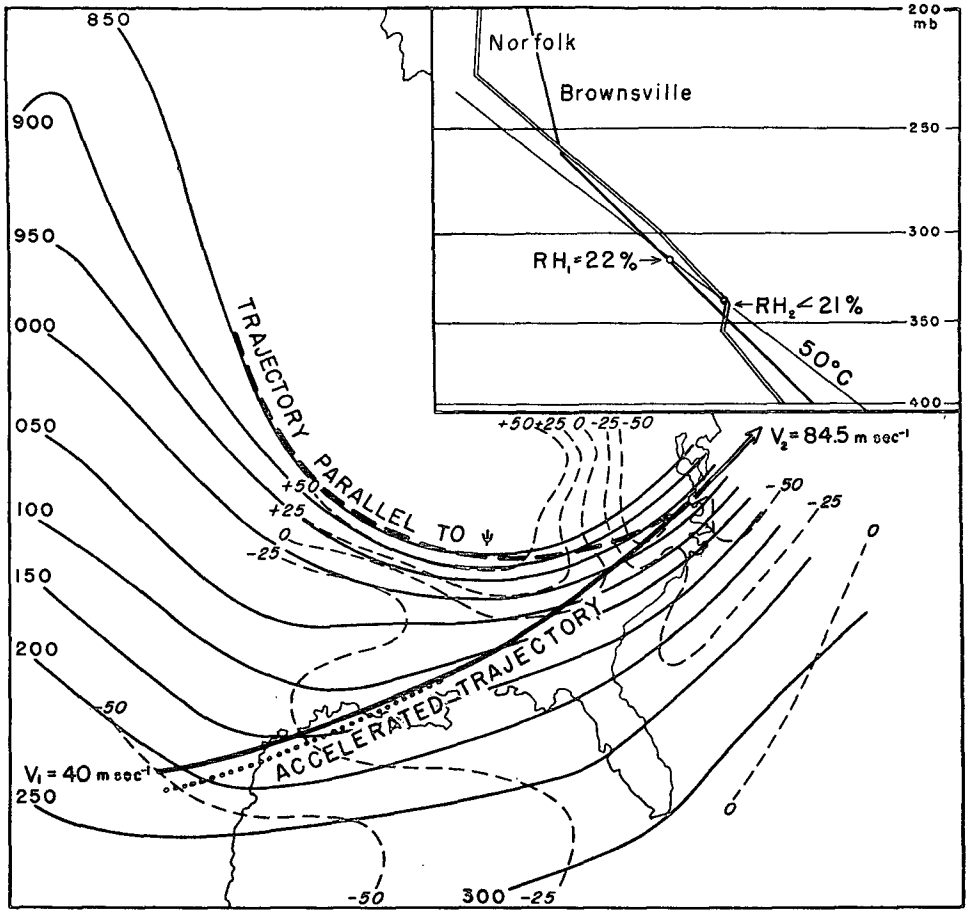

FIG. 7. A portion of the 323K isentropic map at 0000 GCT 2 January 1958 used to demonstrate the construction of an isentropic trajectory. For explanation of diagram see section 4 of text. Soundings in the insert diagram are from Brownsville, Texas at 0000 GCT 2 January 1958 and from Norfolk, Virginia at 1200 GCT 2 January 1958.

An application of the method is demonstrated in fig. 7. The objective was to determine the source region for the air that was observed at Norfolk, Virginia at $\theta = 50C$ or 323K at 1200 GCT 2 January 1958. The values observed at Norfolk, denoted by subscript 2, were

$$\psi_2 = 31910 \times 10^5 \text{ cm}^2 \text{ sec}^{-2}$$

and

$$V_2 = 84.5 \text{ m sec}^{-1}.$$

The light continuous lines in fig. 7 are the isopleths of ψ, labeled with only the last three significant figures, for the map at 0000 GCT 2 January 1958. The dashed lines are the twelve-hour local changes of ψ, labeled with only the last two significant figures.

Eqs. (10) and (11) were first tested along the heavy dashed line by extrapolating upstream for six hours parallel to the ψ_2 isopleth of the 1200 GCT map. This point was then transfered to the 0000 GCT map, and the extrapolation was continued for another six hours to see if both equations could be satisfied. The values of V were everywhere smaller than V_2. At the end of the heavy dashed line, V was only 35 m sec^{-1}; beyond this point, the windspeed decreased rapidly. Although this trajectory may appear reasonable because it satisfies (11), these initial and final values do not satisfy (10). The left side of (10) would be 25 times as large as the right one. To approach a balance, the value of ψ_1 had to be substantially larger. A balance was obtained along the heavy solid line labeled accelerated trajectory. The change in ψ was -307×10^5 cm^2 sec^{-2} of which -277×10^5 cm^2 sec^{-2} produced an increase in kinetic energy corresponding to an initial speed of 40 m sec^{-1} and a final speed of 84.5 m sec^{-1}.

The geostrophic speed at Norfolk as computed from the stream-function analysis was 13.5 m sec^{-1} in excess of the observed speed. A cyclonic curvature is therefore required with a radius of curvature of 6000 km. The dotted line in fig. 7 shows the trajectory implied if this curvature were constant during the twelve hours.

Brownsville, Texas is the radiosonde station nearest to the origin of the trajectory. Its sounding for 0000

GCT 2 January 1958 is shown in the insert diagram of fig. 7 along with the Norfolk sounding 12 hr later. The relative humidity at Brownsville was 22 per cent corresponding to a mixing ratio of 0.07 gm kgm^{-1}. If this was conserved during the descent to Norfolk, the relative humidity would have reduced to 14 per cent, thereby satisfying the <21 per cent observed at Norfolk.

5. Conclusions

The trajectory of an isobaric balloon (the equivalent of an accurately computed isobaric trajectory) is shown to be drastically different from the trajectory of the air if vertical motions and the gradients of vertical motion are large. In extreme but not impossible cases, the two trajectories deviate rapidly in the horizontal differences of $\geqslant 1000$ km in twelve hours, and the curvatures of the two trajectories may be of the opposite sign. It is also shown by equations and examples that the trajectory of an hypothetical isentropic balloon (the equivalent of an accurately computed isentropic trajectory) deviates only slightly from the trajectory of the air for average values of stability and diabatic rates. With low stabilities, the trajectory becomes indeterminate and therefore has the physical significance of a loss of identity of the air parcel by mixing.

An objective method for constructing air trajectories based on the total-energy equation and using data on isentropic surfaces is also developed and demonstrated. This method affords a reliable means of tracing the movement of water vapor, ozone and radioactivity and suggests that the cruder methods in common use may yield misleading results.

REFERENCES

1. Danielsen, E. F., 1959: The laminar structure of the atmosphere and its relation to the concept of a tropopause. *Arch. Meteor. Geophys. Biokl.*, B11, 3H.
2. Brunt, D., 1941: *Physical and dynamical meteorology* (2nd ed.). Cambridge Univ. Press, p. 289.
3. Palmen, E., and C. W. Newton, 1951: On the three-dimensional motions in an outbreak of polar air. *J. Meteor.*, 8, 25–29.